EUROPEAN JOURNAL OF PHARMACEUTICAL SCIENCES 29 (2006) 215–230

available at www.sciencedirect.com

ScienceDirect

journal homepage: www.elsevier.com/locate/ejps

An integrated approach to model hepatic drug clearance

Lichuan Liu[a], *K. Sandy Pang*[a,b,*]

[a] *Department of Pharmaceutical Sciences, Leslie Dan Faculty of Pharmacy, University of Toronto, 19 Russell Street, Toronto, Ontario, Canada M5S 2S2*

[b] *Department of Pharmacology, Faculty of Medicine, University of Toronto, Toronto, Ontario, Canada M5S 2S2*

ARTICLE INFO

Article history:
Received 23 March 2006
Accepted 16 May 2006
Published on line 22 May 2006

Keywords:
Physiologically based pharmacokinetic (PBPK) model
Zonal liver model
Hepatic clearance
Drug transport
Metabolism
Modeling and simulation

ABSTRACT

It has been well accepted that hepatic drug extraction depends on the blood flow, vascular binding, transmembrane barriers, transporters, enzymes and cosubstrate and their zonal heterogeneity. Models of hepatic drug clearances have been appraised with respect to their utility in predicting drug removal by the liver. Among these models, the "well-stirred" model is the simplest since it assumes venous equilibration, with drug emerging from the outflow being in equilibrium with drug within the liver, and the concentration is the same throughout. The "parallel tube" and dispersion models, and distributed model of Goresky and co-workers have been used to account for the observed sinusoidal concentration gradient from the inlet and outlet. Departure from these models exists to include heterogeneity in flow, enzymes, and transporters. This article utilized the physiologically based pharmacokinetic (PBPK) liver model and its extension that include heterogeneity in enzymes and transporters to illustrate how *in vitro* uptake and metabolic data from zonal hepatocytes on transport and enzymes may be used to predict the kinetics of removal in the intact liver; binding data were also necessary. In doing so, an integrative platform was provided to examine determinants of hepatic drug clearance. We used enalapril and digoxin as examples, and described a simple liver PBPK model that included transmembrane transport and metabolism occurring behind the membrane, and a zonal model in which the PBPK model was expanded three sets of sub-compartments that are arranged sequentially to represent zones 1, 2, and 3 along the flow path. The latter model readily accommodated the heterogeneous distribution of hepatic enzymes and transporters. Transport and metabolic data, piecewise information that served as initial estimates, allowed for the unknown efflux and other intrinsic clearances to be estimated. The simple or zonal PBPK model provides predictive views on the hepatic removal of drugs and metabolites.

1. Introduction

The liver is a major site of drug elimination. Hence, an accurate description of hepatic drug clearance is of utmost importance in predicting the pharmacokinetics of drugs. The liver is anatomically and strategically placed behind the intestine, and these act as important first-pass organs for the removal of orally administered drugs. To date, blood flow, vascular (protein and cellular) binding, transporters and metabolic enzymes are regarded as determinants that affect hepatic drug clearance (Pang and Rowland, 1977a,b; Sirianni and Pang, 1997; Liu et al., 2005; Liu and Pang, 2005; Doherty et al., 2006). The unbound drug enters the cell by passive diffusion, or relies on transporters for entry. The intracellular drug is subject to metabolism and/or biliary excretion, and is effluxed back to the blood. In the past, it was assumed

* *Corresponding author*. Tel.: +1 416 978 6164; fax: +1 416 978 8511.
E-mail address: ks.pang@utoronto.ca (K.S. Pang).
0928-0987/$ – see front matter © 2006 Elsevier B.V. All rights reserved.
doi:10.1016/j.ejps.2006.05.007

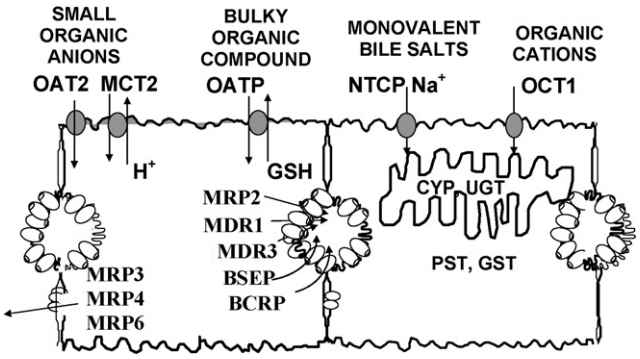

Fig. 1 – Schematic diagram of transport and metabolism of the hepatocyte which shows influx transporters, such as OATP, NTCP, OAT2, OCT1 and MCT2 at the sinusoidal membrane, and efflux transporters such as MRP3, MRP4, and MRP6 at the lateral membrane, and efflux transporters, such as Pgp or MDR1, MRP2, BSEP, BCRP at the canalicular membrane. The enzymes, such as CYP, UGT, PST and GST are present to mediate intracellular metabolism. The figure was modified from Dr. Michael Müller's conception of hepatic transporters.

that drug removal activities of the hepatic enzymes such as the cytochrome P450s (CYPs), UDP-glucuronosyltransferases (UGTs), glutathione *S*-transferases (GSTs), and the sulfotransferases (SULTs) (Parkinson, 2001) or the ATP-dependent canalicular transporters such as P-glycoprotein (Pgp) also named as multidrug resistance protein 1 (MDR1), multidrug resistance associated protein 2 (MRP2), bile salt export pump (BSEP), and breast cancer resistant protein (BCRP) (Keppler and Arias, 1997; Maliepaard et al., 2001; Meier and Stieger, 2002) that account for the irreversible loss of drug due to metabolism and excretion are reflected by the overall rate of drug loss. However, it is increasingly being recognized that metabolism and biliary excretion occur behind the transport barrier. These hepatic transporters include the organic anion transporting polypeptides (OATPs), sodium-dependent taurocholate cotransporting polypeptide (NTCP), organic cation transporters (OCTs), and monocarboxylic acid transporter 2 (MCT2) on the sinusoidal membrane (Hsiang et al., 1999; Kim, 2002; Tirona and Kim, 2002; Mizuno et al., 2003; Trauner and Boyer, 2003) (Fig. 1). Thus, for drugs that do not exhibit flow-limited hepatocellular entry, namely, drugs that are diffusion-limited (Sato et al., 1986; de Lannoy and Pang, 1986, 1987) or drugs that depend on transporter function in bringing drugs into the liver (Pang et al., 1998a; Tirona et al., 1999), sinusoidal transporters could be rate-limiting. Zonal heterogeneities of transporters and metabolic enzymes may further modulate drug disposition in liver (Pang and Stillwell, 1983; Abu-Zahra and Pang, 2000; Tirona and Pang, 1999; Tirona et al., 1999).

Drugs must be able to reach the sinusoidal surface first and be recruited for hepatocellular entry before removal is effected. If the flow to a particular region were absent, metabolism and excretion would not occur. Hence, incomplete mixing of blood from the portal vein (PV, 75%) and hepatic artery (HA, 25%) (Sherman et al., 1996; Takasaki and Hano, 2001; Foley et al., 2003) that result in bypass of the HA or shunting of blood directly from the inlet to the outlet of the sinusoid will reduce drug removal. Moreover, the flow pattern to the liver, the so-called micromixing of the circulation, is of paramount importance that dictates the modeling approach.

1.1. *Models of hepatic clearance*

Hepatic drug clearance, a concept based on urea clearance in the kidney (Möller et al., 1929), has been used to describe hepatic drug removal (Rowland et al., 1973; Wilkinson and Shand, 1975). This parameter is the product of the hepatic blood flow (Q_L) and the extraction ratio (E) of the drug. Various hepatic clearance models have been developed to integrate the factors of flow, binding, transporters and enzymatic activities to predict the drug disposition in liver. Two conventionally used models are "well-stirred" model, which views the liver as a well-stirred compartment with concentration of drug in the liver in equilibrium with that in the emergent blood (Rowland et al., 1973; Pang and Rowland, 1977a), and the "parallel tube" model, which regards the liver as a series of parallel tubes with enzymes distributed evenly around the tubes and the concentration of drug declines along the length of the tube (Winkler et al., 1973) (Fig. 2). Other hepatic clearance models include the series-compartment model (Gray and Tam, 1987), the zonal-compartment or enzyme-distributed model (Pang and Stillwell, 1983; Pang et al., 1986; Abu-Zahra and Pang, 2000), the distributed-model (Bass et al., 1978), and the barrier-limited, variable transit-time model of Goresky and coworkers (Goresky, 1964; Goresky et al., 1973; Geng et al., 1995; Pang et al., 1995).

Distinctly different flow-patterns exist for these models (Fig. 2). The "well-stirred" model assumes bulk flow, and the drug concentration within every part of the liver is identical since the organ is well-stirred, and mixing, denoted by the dispersion number, D_N, is infinite. By contrast, the "parallel-tube" model assumes plug flow, and, under first-order conditions, drug concentration decays in an exponential fashion along the length of the sinusoid, reflecting successive drug recruitment and removal; mixing is non-existent in the lateral direction and between cells, and D_N is zero. Theoretically, the substrate concentration is the unbound drug concentration in the blood leaving the liver for the "well-stirred" model, and is the logarithmic average of the input and output unbound concentrations entering and leaving the liver for the "parallel tube" model. To refine the unrealistically ideal flow condition of "well-stirred" model (100% mixing) and "parallel tube" model (no mixing), a more complicated model, the dispersion model, which displays an intermediate degree of mixing ($D_N > 0$), was developed to include the dispersion relating to the degree of circuitous flow paths of the liver (Perl and Chinard, 1968; Roberts and Rowland, 1985). Theoretically, the substrate concentration in liver for the dispersion model is somewhat in between that for the "well-stirred" and "parallel-tube" models (Fig. 2).

Besides blood flow, vascular binding, transmembrane transport and metabolism are other determinants of hepatic drug clearances. The mathematical expressions relating clearances of these models to hepatic blood flow (Q_L), vascular binding in blood (unbound fraction, f_B) and the hepatocellular enzymatic or excretory activity, in absence of a transmem-

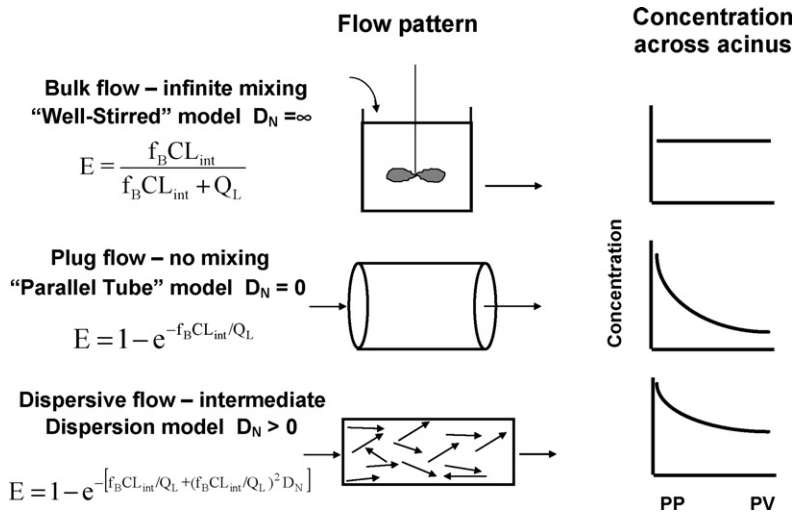

Fig. 2 – Hepatic clearance models based on flow patterns. (A) "Well-stirred" model with infinite mixing (dispersion number $D_N = \infty$); (B) "parallel tube" model without mixing ($D_N = 0$); (C) dispersion model with intermediate mixing ($D_N > 0$). It is shown that hepatic drug extraction ratio (E) is determined by hepatic blood flow (Q_L), vascular binding (unbound fraction in blood, f_B) and the total hepatocellular eliminatory activity (intrinsic clearance, CL_{int}), and D_N in dispersion model, without consideration of the membrane barrier.

brane barrier, have been well described (Pang and Chiba, 1994; Pang, 1995). For all of the models, the concept of the intrinsic clearance, CL_{int}, which relates to the volume of hepatocellular water cleared of drug per unit time, is evoked. For the "well-stirred" model, CL_{int} of the liver is:

$$CL_{int} = \frac{\text{rate of removal}}{[S]} = \frac{(V_{max}[S]/(K_m + [S]))}{[S]} = \frac{V_{max}}{K_m + [S]} \quad (1)$$

Under first-order conditions, this is:

$$CL_{int} = \frac{V_{max}}{K_m} \quad (2)$$

and, for the "parallel-tube" model, the intrinsic clearance under first-order conditions is the length averaged version integrated over the normalized distance of dx over the length of the sinusoid, L:

$$CL_{int} = \frac{\int_0^L (V_{max,x}/K_{m,x})\,dx}{L} \quad (3)$$

The ease of incorporating transporter functions for the "well-stirred" model is readily shown with the physiologically based pharmacokinetic (PBPK) model (de Lannoy and Pang, 1987). To further add heterogeneity of enzymes and transporters (Xu et al., 1993; Kwon and Morris, 1997), zonal models that are able to describe drug metabolism and transport functions in the zones 1, 2, and 3 of the liver (corresponding to periportal, midzonal, and perivenous zones) have been developed (Abu-Zahra and Pang, 2000; Liu et al., 2005).

1.2. *In vitro data*

For model building, it is necessary to investigate each determinant of drug clearance *in vitro*. Drug protein binding data may be obtained *in vitro* by techniques such as equilibrium dialysis or ultrafiltration (Geng et al., 1995). Red blood cell (RBC) distribution may be investigated by mixing drug-containing plasma to blank blood, then accounting for loss of drug in plasma to the RBC by mass balance over time. At some point, equilibrium may be reached. If this takes place over a period of time, RBC binding may be a slow process and may influence hepatic drug removal (Goresky et al., 1975; Pang et al., 1995; Liu et al., 2005).

For metabolic data, the observations have been made at the subcellular or cellular levels, with S9, cytosolic and microsomal fractions or isolated hepatocytes (Tan and Pang, 2001; Lam and Benet, 2004) to obtain the metabolic parameters. Other systems include reconstituted enzyme systems (Miller and Guengerich, 1983), hepatocyte culture (Gomez-Lechon et al., 2004) and tissue slices (Thohan and Rosen, 2002). The data provide *in vitro* K_m and V_{max} and in turn *in vitro* CL_{int}, which is normally used to approximate V_{max}/K_m. However, there are some reported cases that the *in vitro* K_m and V_{max} differed from those *in vivo* (Mistry and Houston, 1987; Pang and Chiba, 1994; Obach, 1999). This occurs especially for the glucuronidation system (Burchell and Coughtrie, 1989; Boase and Miners, 2002; Soars et al., 2002), in which lower values of *in vitro* CL_{int} compared with *in vivo* CL_{int} would be observed unless the UGTs in the microsomes are detergent-activated or when hepatocytes are used instead of microsome (Soars et al., 2002; Lin and Wong, 2002). However, the opposite of higher V_{max} values resulted (Ullrich and Bock, 1984). In addition, the *in vitro* activities of some of the CYPs are often lower than those *in vivo* (Carlile et al., 1999). Care must be exerted to conserve stability of enzymes of *in vitro* preparations.

Transport data are usually acquired from hepatocyte uptake studies in even (Hassen et al., 1996) or zonal cells (Abu-Zahra et al., 2000), or with membrane vesicles prepared from the basolateral or canalicular membrane (Meier and Boyer, 1990). A recently developed sandwich-cultured hepatocyte system (Liu et al., 1999) may also be used. With the

development of molecular engineering, *in vitro* gene expression systems in *Xenopus laevis* oocytes or mammalian cells have been used in transport for the uptake via a single transporter (Meier, 1996; Pang et al., 1998b; Shitara et al., 2002) or uptake and excretion by transporters in doubly transfected systems (Cui et al., 2001; Sasaki et al., 2002, 2004; Spears et al., 2005; Matsushima et al., 2005; Letschert et al., 2005; Mita et al., 2005) or even quadruple transfectant system (Kopplow et al., 2005). Recently, *in silico* method was utilized to identify the pharmacophores of transporters, such as rat Oatp1 and human OATP2 (Chang et al., 2005), from *in vitro* literature data. Multiple indicator dilution (MID) studies may also be used to examine uptake transport clearance through comparison to sucrose, a vascular reference whose distribution represents that of the unbound species, albumin, a vascular reference whose distribution mimics that for the albumin-bound species, or red blood cells, whose distribution is that for the erythrocyte-bound drug species. For drugs that are bound to albumin, a hypothetic reference consisting of the bound fraction and the spaces distributions of sucrose (free species) and albumin (bound species) may be made. The influx coefficient may be ascertained by plotting the logarithmic concentration ratio of the drug/hypothetic reference versus the early time points (Goresky et al., 1975; Pang et al., 1995; Geng et al., 1995). MID studies further reveal the rate constants of sinusoidal efflux and biliary excretion (Geng et al., 1995; Doherty et al., 2006).

In this mini-review, uptake, metabolism and excretion data of enalapril and digoxin *in vitro* and in the perfused rat liver preparation were used to illustrate how *in vitro* data may be used for the description or prediction of clearances *in vivo*. The perfused liver preparation has been used to integrate the *in vitro* data to the organ, in which the architecture of the liver remains intact, and the relationship between the flow and the cell is maintained for recruitment of transporters and enzymes along the direction of flow. At the organ level, the perfused liver preparation provides an integrative platform for investigating the interactions of the determinant of drug clearance. With these model compounds, we will demonstrate that the *in vitro* data are applicable to represent parameters *in vivo* in physiologically based pharmacokinetic (PBPK) liver models. We then make predictions on how changes in transport (influx, efflux or excretion) affect drug metabolism with the models.

2. The single, liver compartment, PBPK model

A simple, physiologically based model for a recirculating liver perfusion system has been developed to include both transporters and enzymes and their associated intrinsic clearances (Sirianni and Pang, 1997). The model is divided into four compartments: the reservoir (R, or blood compartment), liver plasma (PL), liver tissue (L) and bile compartment (bile). The transport clearances across the sinusoidal membrane for drug from hepatic plasma to tissue and from tissue to hepatic plasma are characterized by influx (CL_{influx}) and efflux (CL_{efflux}) clearances, respectively. Drug within the tissue is metabolized by enzymes of intrinsic clearance, $CL_{int,met}$ (V_{max}/K_m for first-order condition). Biliary excretion of drug is a function of the biliary intrinsic clearance, $CL_{int,sec}$, across the canalicular membrane (Fig. 3). With consideration of the hepatic flow rate (Q_L) and protein binding (denoted by f_P for unbound fraction in plasma and f_L for unbound fraction in tissue), Sirianni and Pang solved the clearance terms—$CL_{liver,ex}$, $CL_{liver,met}$, and $CL_{liver,tot}$. As shown in Table 1, the steady-state clearances are complex equations relating not only to flow (Q_L), the unbound fraction in plasma (f_P), the metabolic ($CL_{int,met}$) and secretory ($CL_{int,sec}$) intrinsic clearances but also the influx (CL_{influx}) and efflux (CL_{efflux}) clearances at the basolateral membrane. The unbound fraction in tissue (f_L) was absent, showing that tissue binding is irrelevant in the hepatic drug clearances under first-order condition.

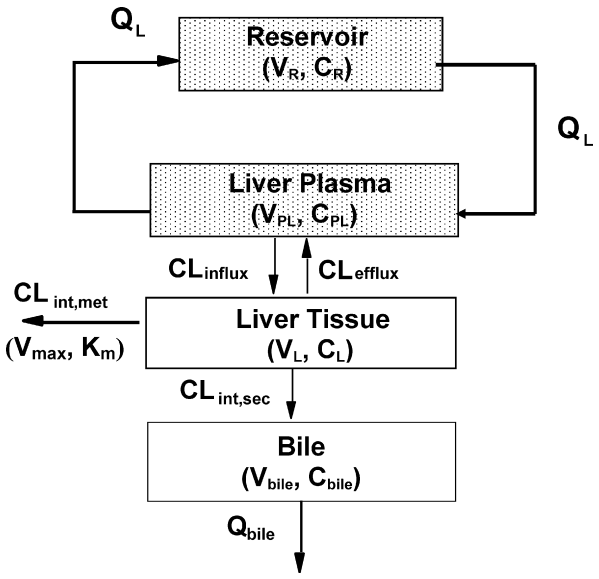

Fig. 3 – A schematic depiction of the liver in a simple, physiological model. The model is divided into four compartments: the reservoir (R, or blood compartment), liver plasma (PL), and liver tissue (L); excretion occurs with drug and metabolite appearing in the bile compartment (bile). Q_L, C, and V represent flow, concentration, and volume, respectively, and are further qualified by the subscripts for the various compartments, whereas the unbound fractions in plasma and liver are denoted by subscripts P and L, respectively. The transport clearances across the sinusoidal membrane for drug from hepatic plasma to tissue and from tissue to hepatic plasma are characterized by influx (CL_{influx}) and efflux (CL_{efflux}) clearances, respectively. Drug within tissue is metabolized by enzymes of intrinsic clearance, $CL_{int,met}$ (V_{max}/K_m for first-order condition). Biliary excretion of drug is a function of the biliary intrinsic clearance, $CL_{int,sec}$, across the canalicular membrane (reproduced from Liu and Pang (2005), with permission).

3. The zonal model

To consider the zonal distribution of transporters and metabolizing enzymes in the liver, a zonal PBPK model consisting of

Table 1 – Solved equations on the biliary excretion clearance, hepatic metabolic clearance, and total hepatic clearance by Sirianni and Pang (1997)

Clearance terms	Solutions for the simple PBPK model	
	CL_{influx} and CL_{efflux} are comparable to Q_L, $CL_{int,met}$ and $CL_{int,sec}$	$CL_{influx} = CL_{efflux} \gg Q_L$, $CL_{int,met}$ and $CL_{int,sec}$
$CL_{liver,ex}$	$\frac{Q_L f_P CL_{influx} CL_{int,sec}}{Q_L(CL_{efflux}+CL_{int,met}+CL_{int,sec})+f_P CL_{influx}(CL_{int,sec}+CL_{int,met})}$	$\frac{Q_L f_P CL_{int,sec}}{Q_L+f_P(CL_{int,sec}+CL_{int,met})}$
$CL_{liver,met}$	$\frac{Q_L f_P CL_{influx} CL_{int,met}}{Q_L(CL_{efflux}+CL_{int,met}+CL_{int,sec})+f_P CL_{influx}(CL_{int,sec}+CL_{int,met})}$	$\frac{Q_L f_P CL_{int,met}}{Q_L+f_P(CL_{int,sec}+CL_{int,met})}$
$CL_{liver,tot}$	$\frac{Q_L f_P CL_{influx}(CL_{int,sec}+CL_{int,met})}{Q_L(CL_{efflux}+CL_{int,met}+CL_{int,sec})+f_P CL_{influx}(CL_{int,sec}+CL_{int,met})}$	$\frac{Q_L f_P (CL_{int,sec}+CL_{int,met})}{Q_L+f_P(CL_{int,sec}+CL_{int,met})}$

These equations are reduced in complexity when $CL_{influx} = CL_{efflux} \gg Q_L$ and $CL_{int,met}$ and $CL_{int,sec}$. Q_L is the plasma flow rate to the liver.

three compartments in series representing zones 1, 2, and 3 in the liver has been developed (Tirona and Pang, 1996; Abu-Zahra and Pang, 2000). This zonal PBPK model encompasses zonal properties of transport, metabolism, and excretion of drug in the periportal (PP or zone 1), midzonal (zone 2) and perivenous (PV or zone 3) regions (Fig. 4). This model describes heterogeneity in basolateral influx transport, denoted as the influx clearances, $CL_{influx1}$, $CL_{influx2}$, and $CL_{influx3}$ within zones 1, 2, and 3, respectively. Similarly, $CL_{efflux1}$, $CL_{efflux2}$, and $CL_{efflux3}$ are the clearances for basolateral efflux, $CL_{int,sec1}$, $CL_{int,sec2}$, and $CL_{int,sec3}$ for biliary excretion (such as Mrp2 for enalapril and Pgp for digoxin), and $CL_{int,met1}$, $CL_{int,met2}$, and $CL_{int,met3}$ for metabolism within zones 1, 2, and 3, respectively (Fig. 4A). In addition, these models may be expanded to include RBC and protein binding (Fig. 4B).

4. Enalapril

The hepatic uptake, metabolism and excretion of enalparil, an angiotensin-converting enzyme (ACE) inhibitor, are shown in Fig. 5. Enalapril exhibits constancy in its binding with albumin (unbound fraction of 0.55 in 4% albumin) (de Lannoy et al., 1989). The simple scheme of involvement of transporters and enzymes in the hepatic disposition of enalapril renders it an ideal model compound to illustrate the competing nature of transporters and metabolic enzymes in hepatic drug processing. Enalapril is taken up by Oatp1 into rat liver (Pang et al., 1998b) and metabolized by the carboxylesterases to enalaprilat in hepatocytes, and the precursor-product pair are excreted via Mrp2 into bile (Pang et al., 2002) (Fig. 5). The uptake clearance of enalapril from homogeneous hepatocytes (Abu-Zahra et al., 2000) yielded a $V_{max\,(influx)}$ and $K_{m\,(influx)}$ for uptake, and the $K_{m\,(influx)}$ was similar to that for the rat organic anion transporting polypeptide 1, Oapt1 (Pang et al., 1998b); these provide the first order uptake clearance, $V_{max\,(influx)}/K_{m\,(influx)}$ (Table 2). Moreover, the uptake of enalapril was evenly distributed within the rat liver, as found by the identical uptake among the homogeneous and zonal rat hepatocytes (Fig. 6 and Table 2). The immunoreactive Oatp1 protein (Abu-Zahra et al., 2000) and Mrp2 (Tirona and Pang, 1999), detected by Western blotting, was homogenously present among zonal hepatocytes (Fig. 7). The $V_{max\,(influx)}$ and $K_{m\,(influx)}$ for enalapril metabolism (Abu-Zahra and Pang, 2000), assessed in 9000 g supernatant derived from zonal cells, showed a higher perivenous abundance (Table 2). Taking all data under consideration, the influx clearance of enalapril is rapid in comparison to that of metabolism.

Taking advantage that analytical solutions existed for the biliary, metabolic, and total clearances based on the single-liver compartmental, PBPK model (Fig. 3), one may proceed to apply the observed clearances from single-pass and recirculating liver perfusion studies (de Lannoy et al., 1993) in order to appraise the biliary intrinsic clearance, a parameter that is not readily available *in vitro*, with the known metabolic *in vitro* parameters. The ratio of the hepatic metabolic and biliary clearances, $CL_{liver,met}/CL_{liver,ex}$, may be shown to equal the ratio of the intrinsic clearances, $CL_{int,met}/CL_{int,ex}$, for the carboxylesterases and Mrp2, respectively (Table 1). From this relationship, an estimate of $CL_{int,ex}$ may be obtained based on the *in vitro* estimate of $CL_{int,met}$. By assigning the CL_{influx} with the hepatocyte uptake data, the unknown CL_{efflux} that matches the observations on total, metabolic, and biliary clearances of enalapril (de Lannoy et al., 1989, 1993) could be obtained from the equations shown in Table 1. Drug efflux occurs rapidly in relation to metabolism (Table 3).

Upon examination of the data with the zonal model comprising of three zones (Fig. 4A) with an even distribution of transporters but a perivenous carboxylesterase for enalapril metabolism, extraction ratio data on enalapril entering via the hepatic artery (HA) at 2 ml/min, with blank perfusate entering via the portal vein (PV) or hepatic vein (HV) at 10 ml/min in the dually perfused liver preparation was 0.12 for HAHV perfusion and 0.77 for HAPV perfusion. suggesting a perivenous preponderance of the carboxylesterases (Pang et al., 1991). Based on the zonal metabolic intrinsic clearances provided by the *in vitro* data (Table 2), optimization of the data to the zonal model provided an efflux clearance, CL_{efflux}, of 9.2 ml/min (Abu-Zahra and Pang, 2000), a value quite similar to that obtained from the simple, PBPK model (Table 3).

5. Digoxin

An abundance of information exists on the transport and metabolism of digoxin (Dg3) in the literatures. The transport of digoxin into hepatocytes is by both passive diffusion and rat Oatp2 expressed in *Xenopus laevis* oocytes (Noé et al., 1997; Guo and Klaassen, 2001; Hagenbuch et al., 2001) or LCC-PK1 cells (Shitara et al., 2002). In the rat liver, digoxin is primarily metabolized by cytochrome P450 3a (Cyp3a) to the di- and mono-digitoxosides as well as digitoxigenin (Harrison

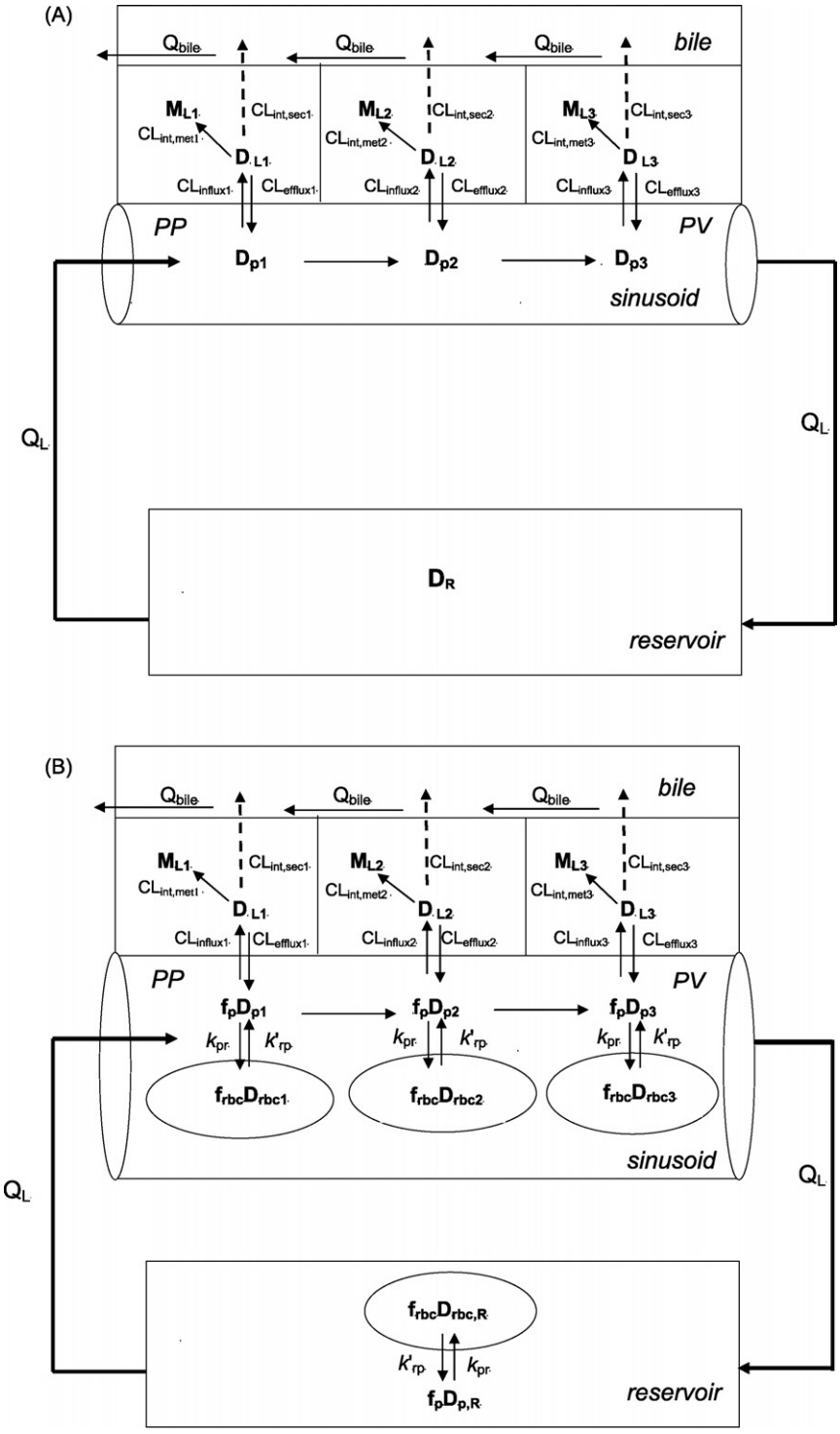

Fig. 4 – The schematic diagram of zonal, physiologically based pharmacokinetic (PBPK) models without (A) or with protein binding and RBC distribution (B). The liver tissue was divided into three zones (PP zone or zone 1, middle zone or zone 2, and PV zone or zone 3) according to the hepatic acinus physiology. $CL_{influxi}$, $CL_{effluxi}$, $CL_{int,meti}$, and $CL_{int,seci}$ were assigned to drug (D) in different zones. M_L was the total formation of metabolite, which included metabolite in reservoir, bile and liver tissue. The RBC partitioning parameters, k'_{rp} and k_{pr}, and protein binding parameter, f_P, from *in vitro* study could be integrated into the PBPK model for fitting and simulation (B).

and Gibaldi, 1976; Salphati and Benet, 1999) and Cyp3a is enriched in PV zone (Oinonen and Lindros, 1995). Digoxin is excreted unchanged into bile by the Pgp (Schinkel et al., 1995) (Fig. 8). In addition, *in vitro* binding data were needed; the unbound fraction in plasma was constant at 0.64 with 1% and 2% albumin over a wide concentration range (Fig. 9A), whereas red cell binding existed with the bovine erythrocytes employed for perfusion (Liu et al., 2005). When the entry and

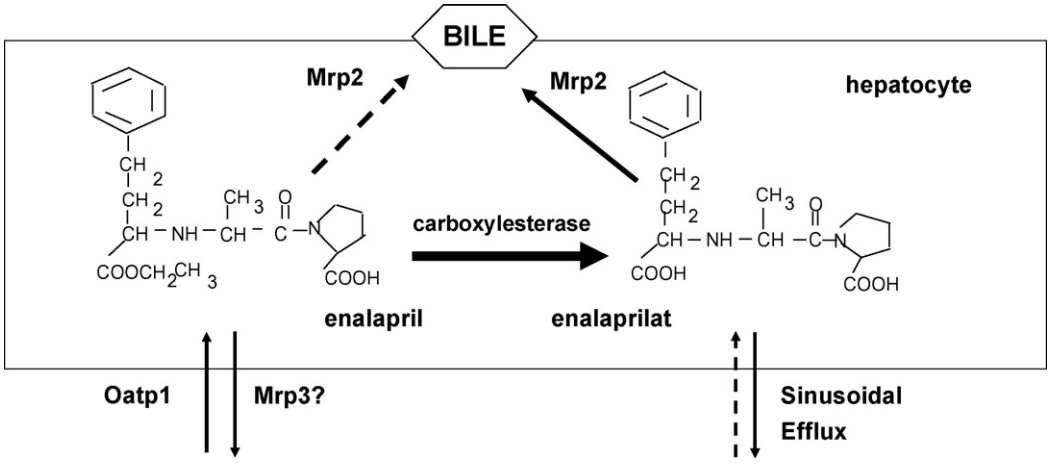

Fig. 5 – The biological fates of enalapril and its metabolite, enalaprilat, in the rat hepatocyte. Enalapril but not its diacid metabolite enalaprilat is taken up by Oatp1 in rat liver, and both compounds are excreted via Mrp2 into bile (Pang et al., 2002). Enalapril is metabolized by the carboxylesterases to enalaprilat. The involvement of transporters and enzymes in the hepatic disposition of enalapril renders the compound as an ideal model substrate for the study of the changes in transporter or enzyme function in liver (reproduced from Liu and Pang (2005), with permission).

efflux rate constants for digoxin permeation into RBC were investigated, rate constants relating to slow processes were obtained (Fig. 9B). In fact, a binding model, that describes the exchange of unbound digoxin between plasma and RBC in relation to the hematocrit (Hct) adequately fitted the digoxin plasma (C_p) and RBC (C_{RBC}) concentration data to arrive at the exchange rate constants between plasma and RBC (k_{pr} and k'_{rp}) (Fig. 9C). Digoxin uptake by zonal (PP and PV) hepatocytes was best described as the sum of a saturable component (K_m and V_{max}) and a non-saturable component (PS_{uptake}), and was identical for both periportal and perivenous hepatocytes (Table 4 and Fig. 10). Other techniques, such as Western blotting and immunofluorescent imaging, confirmed the lack of zonal distribution of Oatp2 and Pgp (Fig. 7) (Liu et al., 2005). Under linear conditions, digoxin uptake clearance by hepatocytes (CL_{uptake}) equals $[V_{max}/(K_m + PS_{uptake})]$, and could be further scaled up to yield the influx clearance, CL_{influx} (Table 4).

Metabolism of digoxin relies on Cyp3a to form Dg2, then Dg1, and Dg0 (Fig. 8). The K_m and V_{max} of Cyp3a for Dg2 formation were reported to be 125 μM and 362 pmol/min/mg, respectively (Salphati and Benet, 1999), and a perivenous distribution of Cyp3a was known (Oinonen and Lindros, 1995).

Data pertaining to *ex vivo* recirculating rat liver perfusion, conducted with Krebs Henseleit buffer (KHB, without RBC and albumin) at 40 ml/min (KHB-perfused liver), or with 20% bovine RBC, 1% bovine serum albumin (BSA) at 10 ml/min (RBC–alb-perfused liver), provided low hepatic clearances for digoxin, and the metabolic and biliary components attributed to metabolism by Cyp3a (metabolic clearance) and excretion by Pgp (biliary clearance) (Table 5). The faster decay profile of Dg3, greater extent of biliary excretion, and the two-fold higher clearance of digoxin (0.244 ml/min/g) in KHB-perfused liver in absence of binding versus the slower clearance in the RBC–alb-perfused liver where binding existed were predicted

Table 2 – Kinetic parameters for metabolism of enalapril by S9 enzymes derived from homogeneous or zonal rat hepatocytes, and the transport constants derived from initial uptake velocities by homogeneous or zonal rat hepatocytes (data of Abu-Zahra and Pang, 2000; Abu-Zahra et al., 2000)

	$K_{m\,(influx)}$ (μM)	V_{max}	$CL_{int} = V_{max}/K_m$ (ml/min/g)
Homogeneous hepatocytes (transport)	344 ± 52	11.0 ± 1.5 nmol/min/10^6 cells or 1425 nmol/min/g liver[a]	4.0
Homogeneous hepatocytes (S9 metabolism)	1308 ± 419	8 ± 3 nmol/min/mg S9 protein or 800 nmol/min/g liver[b]	0.61
Homogeneous hepatocytes: $CL_{influx}/CL_{int,met}$			6.56
Periportal hepatocytes (transport)	461 ± 117	9.5 ± 2.0 nmol/min/10^6 cells	
Periportal hepatocytes (S9 metabolism)	1049 ± 335	5.5 ± 3.1 nmol/min/mg S9 protein or 547 ± 310 nmol/min/g liver	0.52
Perivenous hepatocytes (transport)	441 ± 50	10.4 ± 2.0 nmol/min/10^6 cells	
Perivenous hepatocytes (S9 metabolism)	2612 ± 238	21.0 ± 6 nmol/min/mg S9 protein or 2096 ± 600 nmol/min/g liver	0.82

[a] Based on 130×10^6 cells/g liver (Zahlten and Stratman, 1974).
[b] Based on 100 mg protein/g liver.

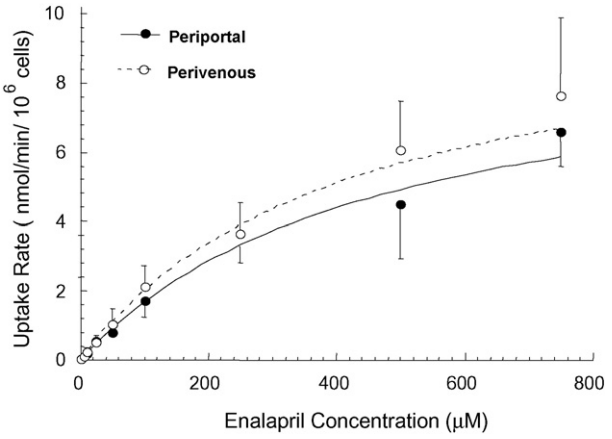

Fig. 6 – Uptake kinetics of enalapril by PP (●) and PV (○) rat hepatocytes in the presence of sodium ion. Data points represent the mean ± S.D. ($n = 4$) of the uptake velocity with increasing concentrations of enalapril. The lines are based on the averaged fitted constants shown in Table 2 for a single saturable uptake component (reproduced from Abu-Zahra et al. (2000), with permission).

well by the zonal, PBPK model (Fig. 11) (Liu et al., 2005). The fit, based on the designated flow rates, volumes, and hematocrit from rat liver perfusion studies, the uptake clearance, CL_{influx} (obtained by scale-up of hepatocyte uptake data), the RBC partitioning constants (k_{pr} and k'_{rp}), and the unbound fraction of digoxin in plasma (f_p), successfully provided the CL_{efflux}, $CL_{int,met}$, $CL_{int,sec}$ and unbound fraction of digoxin in tissue (f_t) (Table 5). It was notable that the metabolite data (summed amounts of Dg2, Dg1 and Dg0) was not used for fitting since mass balance during perfusion could not be ascertained when the liver content was unknown. The metabolic data was furnished by simulation (Fig. 11).

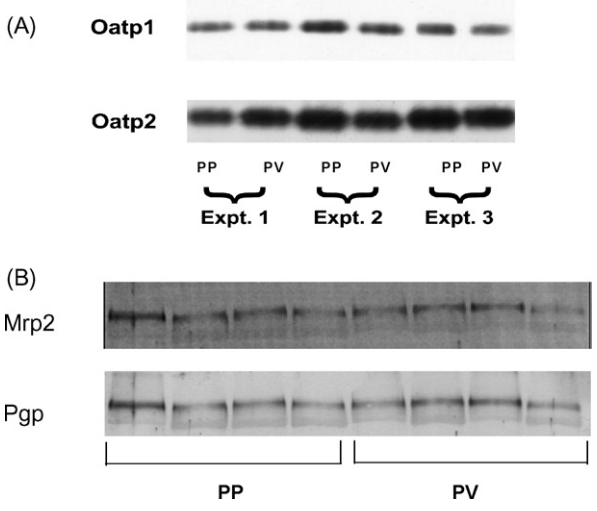

Fig. 7 – Lack of zonal heterogeneity of the rat Oatp1 and Oatp2 for sinusoidal transport (A) and of Mrp2 and Pgp for canalicular efflux (B) in isolated periportal (PP) and perivenous (PV) rat hepatocytes, shown by Western blotting (reproduced from Tirona and Pang (1999) and Liu et al. (2005), with permission).

Table 3 – Estimation of the efflux (CL_{efflux}), metabolic intrinsic clearance ($CL_{int,met}$) and secretory intrinsic clearance ($CL_{int,sec}$) parameters based on the simple PBPK (Fig. 3) for clearances observed in the single-pass perfused rat liver preparation[a]

	Observed data	Predictions
Hepatic metabolic clearance, $CL_{liver,met}$ (ml/min/g)	0.345[a]	0.345
Biliary clearance, $CL_{liver,ex}$ (ml/min/g)	0.022[a]	0.022
Total hepatic clearance, $CL_{liver,tot}$ (ml/min/g)	0.366[a]	0.367
$CL_{liver,met}/CL_{liver,ex} = CL_{int,met}/CL_{int,sec}$	15.7[b]	
$CL_{int,met}$ *in vitro* (ml/min/g)	0.61[c]	
Calculated $CL_{int,sec}$ (ml/min/g)	0.039[b]	
CL_{influx} (ml/min/g)	4.00[d]	
CL_{efflux} (ml/min/g)		1.46[e]
$C_{T,ss}/C_{P,ss}$	1.5–19[f]	
$C_{T,ss,u}/C_{P,ss,u}$		1.9[g]
$CL_{influx}/CL_{int,met}$	6.56	
CL_{influx}/CL_{efflux}	2.7	

[a] Based on data of de Lannoy et al. (1993).
[b] Based on equations in Table 1.
[c] *In vitro* S9 data of Abu-Zahra et al. (2000) (from Table 2).
[d] *In vitro* hepatocyte data of Abu-Zahra and Pang (2000) (from Table 2).
[e] From fit to PBPK model.
[f] Observed by Pang et al. (1991).
[g] $CL_{influx}/(CL_{efflux} + CL_{int,met} + CL_{int,sec})$.

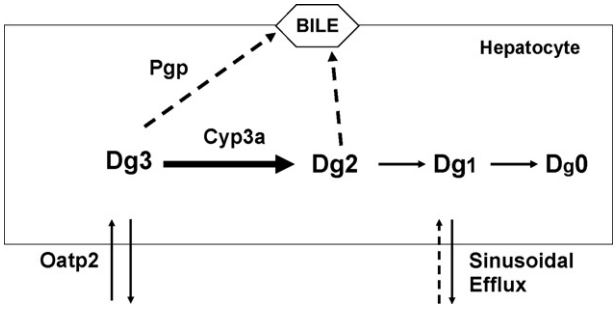

Fig. 8 – The fates of digoxin (Dg3) and its metabolites, Dg2, Dg1, and Dg0 (di-digitosoxide, mono-digitosoxide, and digitoxigenin) in the rat hepatocyte. Dg3 is taken up by Oatp2 in rat liver, and is excreted via Pgp into bile. Dg3 is metabolized by Cyp3a to Dg2, Dg1, and Dg0 (Salphati and Benet, 1999). The involvement of transporters and enzymes in the hepatic disposition of Dg3 renders the compound ideal for the study of the changes in transporter or enzyme function in liver.

6. Simulations

A useful strategy is to perform simulations to predict various outcomes. Meaningful information is readily gathered from the simulations to demonstrate the competing nature of transporters and metabolic enzymes (Table 6). With the above models (Figs. 3 and 4) and parameter values (Tables 3 and 5),

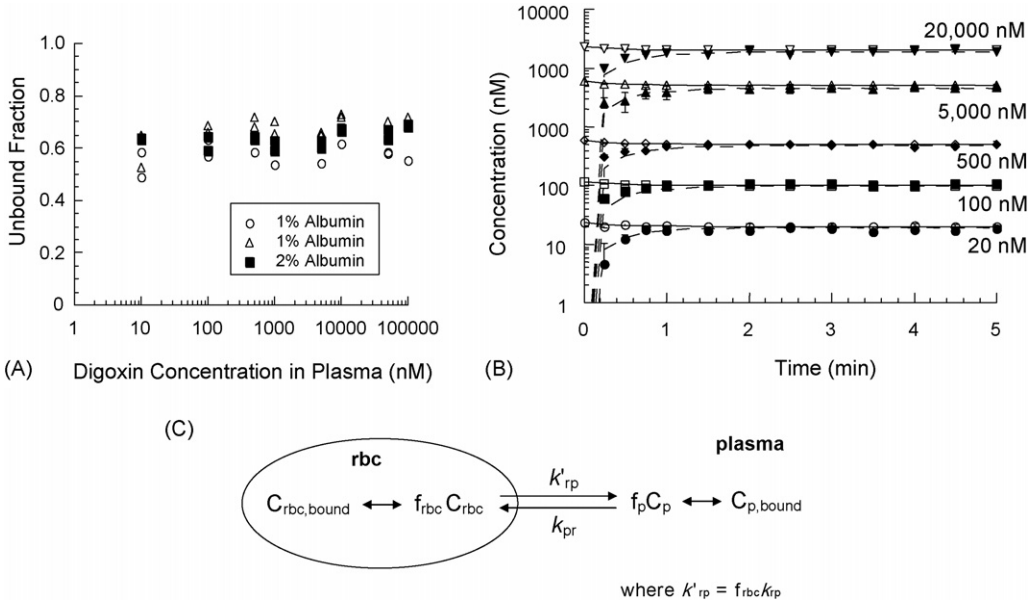

Fig. 9 – (A) Concentration-independent binding of digoxin to 1% or 2% albumin (the unbound fraction in plasma (f_P) averaged 0.64 ± 0.03). (B) Distribution of Dg3 into RBC. After admixture of blank perfusate (40%-RBC, 1%-albumin perfusate) to 0%-RBC and 1%-albumin perfusate containing [^{3}H]- and unlabeled digoxin, a gradual accumulation of Dg3 into RBC was observed. The solid symbols are concentrations in RBC and open symbols are concentrations in plasma perfusate. The lines represent optimized fits to the entire data set to the model shown in (C), with the on and off rate constants, k_{pr} (0.468 ± 0.021 min^{-1}) and k'_{rp} (1.81 ± 0.12 min^{-1}). (C) The model describing the exchange of unbound digoxin between RBC and plasma (where f_{RBC} is the unbound fraction in RBC, which, when multiplied to the total concentration in RBC, C_{RBC}, yields $C_{RBC,u}$ or unbound drug concentrations in RBC; $C_{p,b}$ and $C_{p,u}$ are bound and unbound concentrations in plasma). The exchange of Dg3 unbound drug species between the red cell and plasma is denoted by the rate constants, k_{rp} and k_{pr}, and k'_{rp} is used to denote $f_{RBC}k_{rp}$ since binding within RBC is unknown (reproduced from Liu et al. (2005), with permission).

simulations may be performed for linear or non-linear conditions, or when one of the clearances (influx, efflux, metabolic intrinsic, or excretory intrinsic clearance) is altered. From the simulations, general trends with respect to changes in the influx or efflux clearance, or the metabolic or excretory intrinsic clearance on the total, metabolic, and excretion clearance are found. These trends are identical for the simple and zonal PBPK models (Table 6), and the models are invaluable to illustrate the interplay of transporters and enzymes in hepatic drug processing (Sirianni and Pang, 1997; Liu and Pang, 2005; Liu et al., 2005). The condition of $CL_{int,sec}$ as zero mimics the condition for the Eisai hyperbilirubinemic rat (EHBR) liver that lacks Mrp2 which excretes enalapril (Pang et al., 2002). When the influx clearance is reduced while maintaining the CL_{efflux}, $CL_{int,met}$, and $CL_{int,sec}$ constant, the biliary, metabolic, and total clearances all decreased (Table 6); the converse is true when CL_{influx} is increased. Upon reduction of the efflux clearance, the biliary, metabolic, and total clearances are expected to be all increased; again the converse is true when CL_{efflux} is increased (Table 6). The ratio of the metabolic/excretion or metabolic intrinsic/excretory intrinsic clearances remained constant in spite of the changes of CL_{influx} and CL_{efflux}. Generally speaking, an increase in the intrinsic clearance of one elimination pathway leads to a decrease in the observed clearance of the alternate pathway, and the total clearance is increased. By contrast, a decrease in intrinsic clearance of one pathway leads to an observed increased clearance of the alternate pathway because of compensatory mechanism

Table 4 – *In vitro* metabolism and transport data on digoxin in the rat hepatic microsome and isolated zonal hepatocytes[a]

	K_m[b] (nM)	V_{max}[b] (pmol/min/mg)	PS_{uptake}[c] (μl/min/mg)	CL_{int} (μl/min/mg)
Metabolism	125	362		2.90
Periportal hepatocytes (n = 4)	180 ± 112	13 ± 8	9.2 ± 1.3	83 ± 29[d]
Perivenous hepatocytes (n = 4)	390 ± 406	18 ± 4.9	10.7 ± 2.5	111 ± 80[d]

[a] Metabolic data from Salphati and Benet (1999); uptake data by periportal and perivenous isolated rat hepatocytes, best described by the sum of a saturable and a non-saturable components, were taken from Liu et al. (2005).
[b] Saturable component.
[c] Non-saturable or linear uptake clearance.
[d] Total hepatocyte uptake clearance equals ($V_{max}/K_m + PS_{uptake}$).

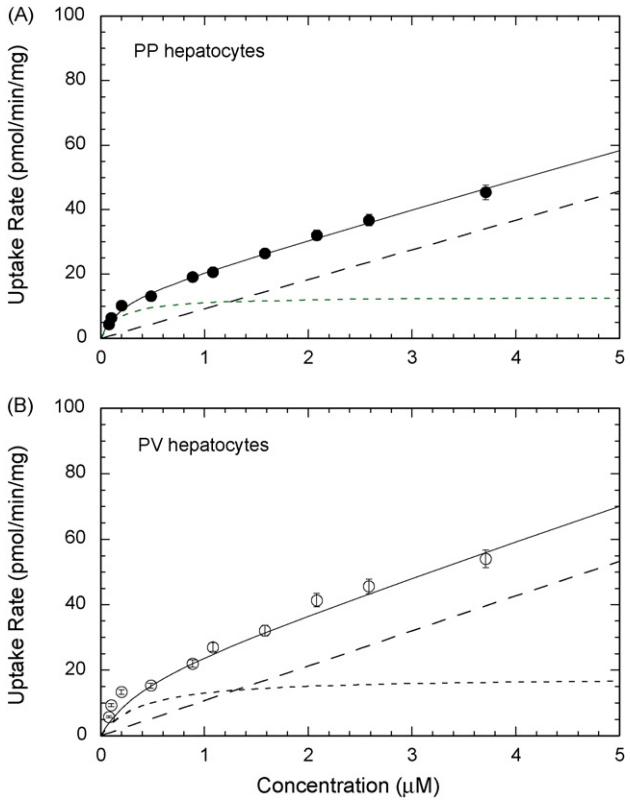

Fig. 10 – Rates of digoxin uptake by (A) PP and (B) PV isolated rat hepatocytes at different concentrations ($n = 4$): the solid lines, fitted lines with an optimal weighting scheme of 1/observation^2, are a sum of a saturable component (small dash lines) and a non-saturable component (medium dash lines) (reproduced from Liu et al. (2005), with permission).

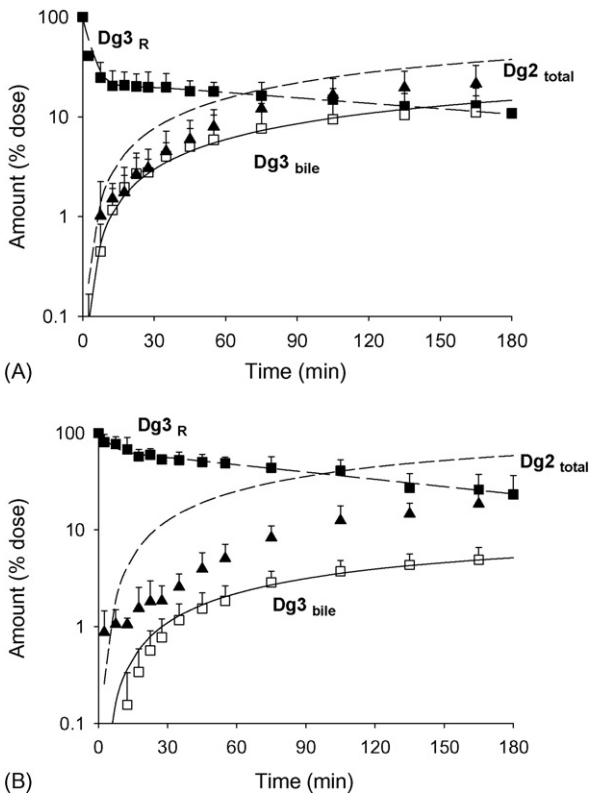

Fig. 11 – Fits of the Dg3 data in reservoir ($Dg3_R$) and bile ($Dg3_{bile}$) to the zonal, PBPK model (Fig. 4) for the KHB-perufsed (without binding) (A) and RBC–alb-perfused (with binding) (B) livers. The solid triangle symbols are the summed amounts of Dg2 in reservoir and bile (% dose) that were underestimations of the total Dg2 formed ($Dg2_{total}$) (reproduced from Liu et al. (2005), with permission).

Table 5 – Assigned and fitted parameters to zonal model shown in Fig. 4, based on the fit to the average data

	KHB-perfused livers	RBC–alb-perfused livers (20% RBC–1% albumin)	Forced fitting
Q_L (ml/min/g)	3.58	0.811	
Hct	0	0.142	
V_R (ml/g)	14.6[a]	12.2	
V_S (ml/g)	0.149[b]	0.149	
V_L (ml/g)	0.663[c]	0.663	
k'_{rp} (min^{-1})	0	1.81	
k_{pr} (min^{-1})	0	0.468	
f_P	1	0.64[d]	
CL_{influx} (ml/min/g)	12.1[e]	12.1	12.1
CL_{efflux} (ml/min/g)	8.52 ± 54.0[f] (9.28 ± 177)[g]	14.3 ± 388 (14.1 ± 204)	11.4 ± 776 (16.0 ± 262)
$CL_{int,met}$ (ml/min/g)	0.143 ± 0.901 (0.153 ± 2.91)	0.202 ± 5.49 (0.197 ± 2.84)	0.127 ± 8.66 (0.226 ± 3.70)
$CL_{int,sec}$ (ml/min/g)	0.054 ± 0.345 (0.059 ± 1.13)	0.017 ± 0.469 (0.017 ± 0.250)	0.025 ± 1.68 (0.046 ± 0.744)
f_t	0.018 ± 0.116 (0.017 ± 0.321)	0.051 ± 1.40 (0.052 ± 0.749)	0.034 ± 2.33 (0.019 ± 0.311)

[a] Mean of reservoir volume normalized to averaged liver weight.
[b] Sinusoidal blood volume of liver, taken from Pang et al. (1988).
[c] Cellular water space of liver, taken from Pang et al. (1988).
[d] Unbound fraction in plasma (1 and 2% albumin) for 0.01–100 μM digoxin.
[e] Calculated from data of Table 6, the data were scaled-up with the scaling factor (α/β; where α is 1.25×10^8 cells/g liver and β is 1×10^6 cells/mg protein) (Tirona and Pang, 1999).
[f] Fitted parameter and standard deviation when the metabolic activity, $CL_{int,met}$, was distributed heterogeneously (10:30:60% of total intrinsic clearance at zones 1, 2 and 3, respectively).
[g] Fitted parameter and standard deviation when $CL_{int,met}$ was distributed homogeneously in zones 1, 2 and 3.

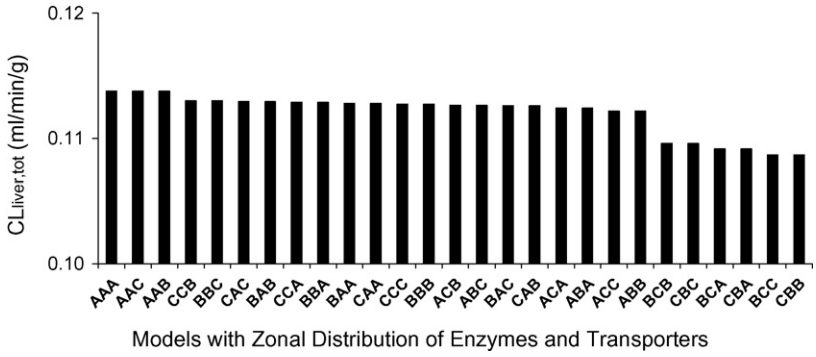

Fig. 12 – The effects of enzyme and transporter heterogeneity on total hepatic clearance ($CL_{liver,tot}$) from simulations in zonal PBPK model (Fig. 4). For simplicity, each model is assigned three letters, e.g. ACB or AAA [the first, second, and third letters of the model are used to describe the distribution of sinusoidal transport, enzyme, and canalicular transporter or the distributions of the influx and efflux clearances (CL_{influx} and CL_{efflux}), metabolic ($CL_{int,met}$) and secretory ($CL_{int,sec}$) intrinsic clearances, respectively]. "A" represents an even distribution as (1:1:1 among all zones), "B" denotes preferential PV distribution (1:3:6 among zones 1, 2, and 3), and "C" is preferential PP distribution (6:3:1, in zone 1, 2, and 3). The various distributions resulted in 27 possible combinations and were arranged in a descending values of $CL_{liver,tot}$.

(a see-saw phenomenon), due to increase in intracellular substrate concentration.

Needless to say, the simulations provide mechanistic insight into the rate-limiting factor controlling hepatic drug clearance. To address the effect of enzyme and transporter heterogeneity on hepatic clearances, patterns on transporter and enzyme distribution were used for simulation with the zonal PBPK model. For simplicity, even distribution (1:1:1, denoted as A), preferential PV distribution (1:3:6, denoted as B), and preferential PP distribution (6:3:1, denoted as C) in zone 1, 2, and 3 were assigned to influx and efflux clearances (CL_{influx} and CL_{efflux}), metabolic ($CL_{int,met}$) and secretory ($CL_{int,sec}$) intrinsic clearances, respectively. The first letter of the model, e.g. "A" in "ABC" denotes the distribution of the sinusoidal influx and efflux transporters that are assumed to share the same distribution; the second letter is used to denote the distribution of enzymes, and the third, for the distribution of canalicular transporters. The various distributions resulted in 27 possible combinations. All of the possible distribution patterns were used to simulate digoxin disposition with the zonal PBPK model shown in Fig. 4B, and the best

Table 6 – Similar trends in the total hepatic, metabolic, and excretion clearance when the influx, efflux, metabolic, or secretory intrinsic clearances are changed under the linear conditions, for both the single liver compartment PBPK model (Fig. 3) and the zonal PBPK model (Fig. 4)

	$CL_{liver,tot}$	$CL_{liver,met}$	$CL_{liver,ex}$
Increase CL_{influx}	Increase	Increase	Increase
Decrease CL_{influx}	Decrease	Decrease	Decrease
Increase CL_{efflux}	Decrease	Decrease	Decrease
Decrease CL_{efflux}	Increase	Increase	Increase
Increase $CL_{int,met}$	Increase	Increase	Decrease
Decrease $CL_{int,met}$	Decrease	Decrease	Increase
Increase $CL_{int,sec}$	Increase	Decrease	Increase
Decrease $CL_{int,sec}$	Decrease	Increase	Decrease
Increase f_P	Increase	Increase	Increase

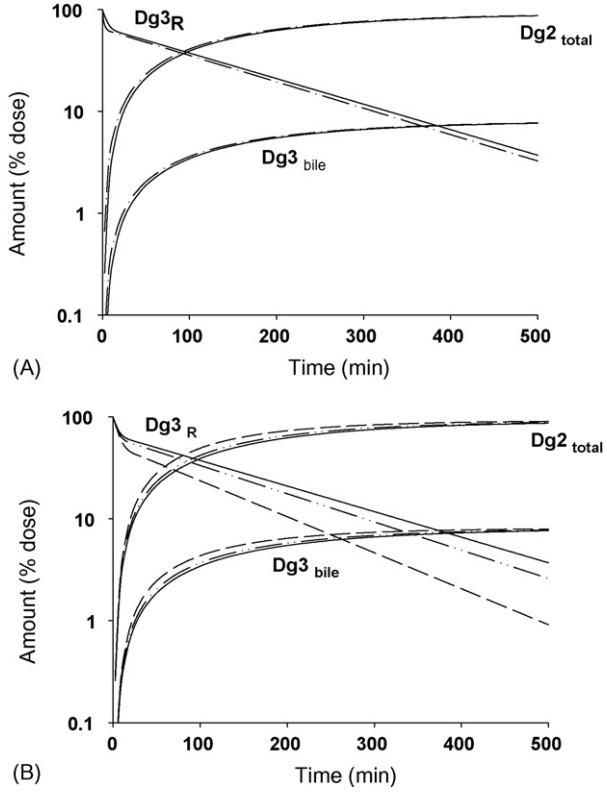

Fig. 13 – Simulations of the effect of flow rate (A) or binding (B) on Dg3 in reservoir ($Dg3_R$), bile ($Dg3_{bile}$) and total Dg2 formation ($Dg2_{total}$) with the PBPK model (Fig. 4B), based on parameter values for the RBC–alb-perfused livers (Table 5, third column, and metabolic activity was evenly distributed). (A) The flow rate was increased from 10 (solid line) to 40 ml/min (dash-dot line). (B) The on and off binding constants for digoxin with red cell were set as zero ($k'_{rp} = k_{pr} = 0$) (—·—), and binding to BSA was further set as absent ($f_P = 1$) (— – —) (reproduced from Liu et al. (2005), with permission).

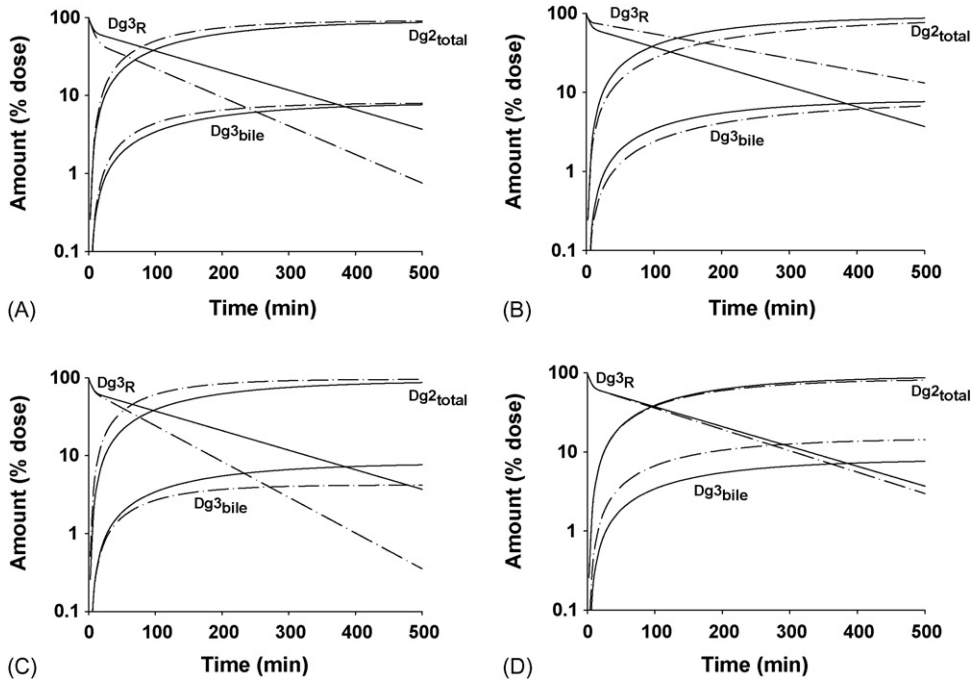

Fig. 14 – Simulations of the effect of doubling the CL_{influx} (A), CL_{efflux} (B), $CL_{int,met}$ (C), and $CL_{int,sec}$ (D) on Dg3 in reservoir ($Dg3_R$), bile ($Dg3_{bile}$) and total Dg2 formation ($Dg2_{total}$) with PBPK model (Fig. 4B), based on the parameter values from RBC–alb-perfused livers (Table 5, third column, even distribution of $CL_{int,met}$). The changes from the original, controlled condition (—) were denoted as (—·—) (reproduced from Liu et al. (2005), with permission).

and worst enzyme/transporter patterns could be identified (Fig. 12).

Simulation with the zonal PBPK model showed that increasing the blood flow rate from 10 to 40 ml/min failed to perturb the concentration-profile and decay processes, and both excretion and metabolism of digoxin remained similar (Fig. 13A). Whereas when red cell binding was set as non-existent ($k_{pr} = k'_{rp} = 0$), the decay profile of digoxin was more rapid, and all clearance values: excretory and metabolic, were notably increased (Fig. 13B). When albumin binding was further set as zero ($f_P = 1$), steeper changes in decay were observed, and all of the clearance values were increased further (Fig. 13B), showing that binding and not flow affected the clearance of digoxin among the liver preparations. To investigate the interrelationship of the transporters and the metabolic enzymes in this zonal PBPK model, the intrinsic clearance, CL_{influx}, CL_{efflux}, $CL_{int,met}$ or $CL_{int,sec}$, was doubled in individual simulations. The results (Fig. 14) showed those trends based on zonal PBPK model were similar to those in previous simple PBPK model. An increase in influx clearance increased the metabolic, excretory, and total hepatic clearances, whereas a decrease in influx clearance would bring about the opposite effect. An increase in efflux clearance would bring about a decrease in the metabolic, excretory, and total hepatic clearances, whereas a decrease in efflux clearance would bring the opposite effects. An increase in the metabolic intrinsic clearance would reduce total clearance but increase the alternate, biliary clearance, whereas a decrease in the metabolic intrinsic clearance would bring about a decrease in total clearance and increase the biliary clearance (Table 6). These compensatory mechanisms confirm the competing nature of transporters and metabolic enzymes and offer identical trends to those predicted by the PBPK model.

6.1. *Modeling of other data sets*

The same model (Fig. 3) may be used to describe other data sets, even though non-linear metabolism or excretion existed. Morphine (M) glucuronidation and excretion was found to be non-linear at concentrations ranging from 9 to 474 μM in the single-pass perfused rat liver preparation. For morphine and its morphine 3β-glucuronide metabolite (M3G), modest binding existed with 4% BSA (unbound fractions of 0.89 ± 0.07 and 0.98 ± 0.09, respectively), and there was partitioning of M into red blood cells (red cell/plasma concentration ratio of 1.36) (Doherty et al., 2006). Exploration of uptake of M in zonal hepatocytes revealed that uptake clearances (1.5 ml/min/g) were similar and there was lack of concentration dependence. Transport of M3G, ascertained in multiple indicator dilution (MID), uncovered a low and concentration-independent influx clearance (<10% of flow rate) at various input M3G concentrations (10–262 μM). There was negligible biliary excretion of M3G. By contrast, M3G appeared abundantly in both perfusate and bile in single pass perfusion studies of the precursor, M, and revealed a biliary clearance of formed M3G that was 12.3-fold that of preformed

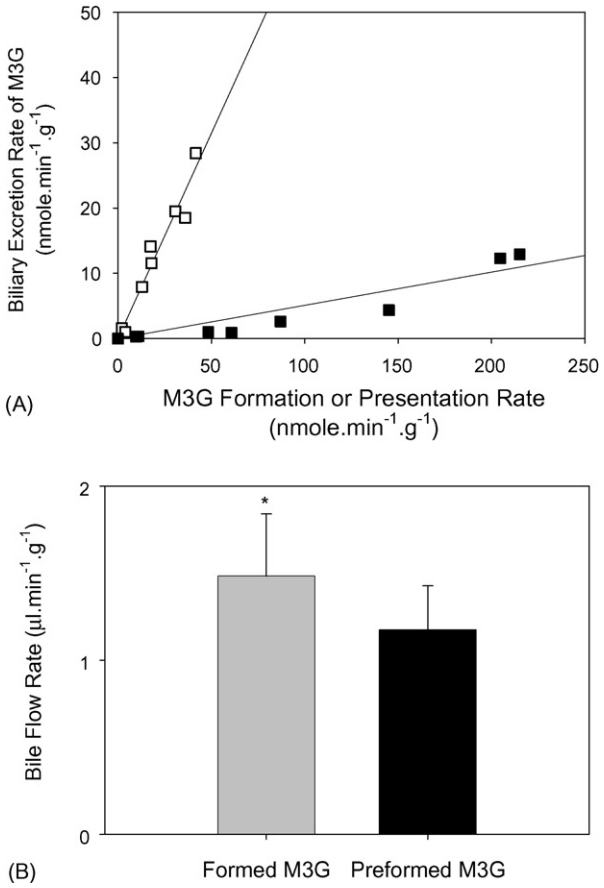

Fig. 15 – (A) Plots of the biliary excretion rates of M3G vs. input rates with M3G administration (■) and vs. the formation rates of M3G resulting from M administration (□). The extraction ratio, estimated from the slope, was higher for formed M3G (0.63) than for the preformed M3G (0.051). (B) The bile flow rate during the M experiments was higher than that for the preformed M3G studies due to the choleretic properties of M3G; the asterisk denotes $P < 0.05$ (reproduced from Doherty et al. (2006), with permission).

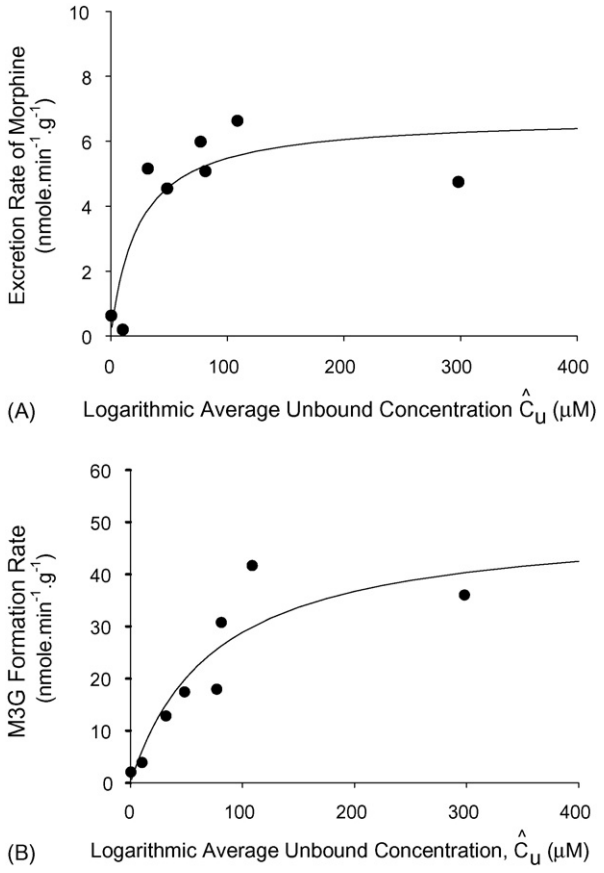

Fig. 16 – The excretion rate of morphine in bile (A) and the rates of M3G formation (summed rates of M3G in perfusate and bile) (B), plotted against the logarithmic average of the unbound input and output concentration of M. Michaelis-Menten kinetics was observed for the excretion (A) and metabolism (B) of M. The lines represented fitted lines upon non-linear regression of biliary excretion (A) and metabolism (B) of M against the logarithmic average of the unbound input and output concentration. A weighting of unity best described the data (reproduced from Doherty et al. (2006), with permission).

M3G, suggesting a sinusoidal, diffusional barrier for M3G (Fig. 15).

With the transport and binding data for M and M3G in hand, the metabolic and excretory data of M were fit to the model (Fig. 3) to yield the V_{max} and K_m for metabolism and excretion (Doherty et al., 2006). M removal mechanisms were saturable, with a $K_{m,met}$ of 52.2 μM and $V_{max,met}$ of 58.8 nmol/min/g for metabolism, and a $K_{m,ex}$, of 41.2 μM and $V_{max,ex}$ of 8.1 nmol/min/g for excretion. The intrinsic clearance (V_{max}/K_m) so obtained revealed that uptake was much faster than metabolism and excretion. Since sinusoidal transport was not rate-limiting for M removal, these kinetic constants may also be approximated upon regression of the rate of metabolism or excretion against the logarithmic unbound concentration of M (Fig. 16) (Doherty et al., 2006).

7. Conclusions

The use of PBPK modeling successfully allowed the fruitful integration of *in vitro* data into whole organ hepatic drug processing. We have illustrated these principles with enalapril, digoxin, and morphine for which we investigated the *in vitro* uptake, metabolism, and binding, and in the perfused rat liver preparation. These models allow the rate-limiting step of drug clearance to be discerned. The interplay of transporters and enzymes are readily demonstrated. The power of physiologically based pharmacokinetic (PBPK) model shows that knowledge on the physicochemical properties of the drug and the physiology, biochemistry, and anatomy of organ and whole body could be integrated into the model. Moreover, the influence of the various determinants of drug disposition in the body or organ could be appraised by computer simulation. From the summarized work, it is evident that the simple

PBPK model has predictive properties in presenting integrative views on hepatic drug extraction, whereas the zonal liver model, which is based on hepatic acinus physiology, is superior since it is able to describe the attendant heterogeneities of transporters and enzymes. *In vitro* hepatocyte transport and metabolic data, and information on the zonal distribution of transporters and enzymes are building blocks of the (zonal) PBPK model. Although enalapril and digoxin were chosen as the examples because of the existence of *in vitro* data on transport and metabolism and *ex vivo* liver perfusion data in our laboratory, the developed concepts are pertinent to all drugs and allow us to quantitatively explain the effects of blood flow, vascular binding, transport and metabolism on hepatic drug disposition. In summary, the zonal PBPK model is an invaluable tool in understanding the various mechanisms underlying hepatic drug disposition.

Acknowledgments

The work was supported by the Canadian Institute for Health Research, MOP64350. LL was supported by the Ontario Graduate Scholarship.

REFERENCES

Abu-Zahra, T.N., Pang, K.S., 2000. Effect of zonal transport and metabolism on hepatic removal: enalapril hydrolysis in zonal, isolated rat hepatocytes *in vitro* and correlation with perfusion data. Drug Metab. Dispos. 28, 807–813.

Abu-Zahra, T.N., Wolkoff, A.W., Kim, R.B., Pang, K.S., 2000. Uptake of enalapril and expression of organic anion transporting polypeptide 1 in zonal, isolated rat hepatocytes. Drug Metab. Dispos. 28, 801–806.

Bass, L., Robinson, P., Bracken, A.J., 1978. Hepatic elimination of flowing substrates: the distributed model. J. Theor. Biol. 72, 161–184.

Boase, S., Miners, J.O., 2002. *In vitro–in vivo* correlations for drugs eliminated by glucuronidation: investigations with the model substrate zidovudine. Br. J. Clin. Pharmacol. 54, 493–503.

Burchell, B., Coughtrie, M.W., 1989. UDP-glucuronosyltransferases. Pharmacol. Ther. 43, 261–289.

Carlile, D.J., Hakooz, N., Bayliss, M.K., Houston, J.B., 1999. Microsomal prediction of *in vivo* clearance of CYP2C9 substrates in humans. Br. J. Clin. Pharmacol. 47, 625–635.

Chang, C., Pang, K.S., Swaan, P.W., Ekins, S., 2005. Comparative pharmacophore modeling of organic anion transporting polypeptides: a meta-analysis of rat Oatp1a1 and human OATP1B1. J. Pharmacol. Exp. Ther. 314, 533–541.

Cui, Y., Konig, J., Keppler, D., 2001. Vectorial transport by double-transfected cells expressing the human uptake transporter SLC21A8 and the apical export pump ABCC2. Mol. Pharmacol. 60, 934–943.

de Lannoy, I.A.M., Pang, K.S., 1986. A commentary: presence of a diffusional barrier on metabolite kinetics. Enalaprilat as a generated versus preformed metabolite. Drug Metab. Dispos. 14, 513–520.

de Lannoy, I.A.M., Pang, K.S., 1987. Effect of diffusional barriers on drug and metabolite kinetics. Drug Metab. Dispos. 15, 51–58.

de Lannoy, I.A., Barker III, F., Pang, K.S., 1993. Formed and preformed metabolite excretion clearances in liver, a metabolite formation organ: studies on enalapril and enalaprilat in the single-pass and recirculating perfused rat liver. J. Pharmacokinet. Biopharm. 21, 395–422.

de Lannoy, I.A., Nespeca, R., Pang, K.S., 1989. Renal handling of enalapril and enalaprilat: studies in the isolated red blood cell-perfused rat kidney. J. Pharmacol. Exp. Ther. 251, 1211–1222.

Doherty, M.M., Poon, K., Tsang, C., Pang, K.C., 2006. Transport is not rate-limiting in morphine glucuronidation in the single pass perfused rat liver preparation. J. Pharmacol. Exp. Ther., February 7 [Epub ahead of print].

Foley, D.P., Ricciardi, R., Traylor, A.N., McLaughlin, T.J., Donohue, S.E., Wheeler, S.M., Meyers, W.C., Quarfordt, S.H., 2003. Effect of hepatic artery flow on bile secretory function after cold ischemia. Am. J. Transplant. 3, 148–155.

Geng, W.P., Schwab, A.J., Goresky, C.A., Pang, K.S., 1995. Carrier-mediated uptake and excretion of bromosulfophthalein-glutathione in perfused rat liver: a multiple indicator dilution study. Hepatology 22, 1188–1207.

Gomez-Lechon, M.J., Donato, M.T., Castell, J.V., Jover, R., 2004. Human hepatocytes in primary culture: the choice to investigate drug metabolism in man. Curr. Drug Metab. 5, 443–462.

Goresky, C.A., 1964. Initial distribution and rate of uptake of sulfobromophthalein in the liver. Am. J. Physiol. 207, 13–26.

Goresky, C.A., Bach, G.G., Nadeau, B.E., 1975. Red cell carriage of label. Its limiting effect on the exchange of materials in the liver. Circ. Res. 36, 328–351.

Goresky, C.A., Bach, G.C., Nadeau, B.E., 1973. On the uptake of materials by the intact liver. The transport and net removal of galactose. J. Clin. Invest. 52, 991–1009.

Gray, M.R., Tam, Y.K., 1987. The series-compartment model for hepatic elimination. Drug Metab. Dispos. 15, 27–31.

Guo, G.L., Klaassen, C.D., 2001. Protein kinase C suppresses rat organic anion transporting polypeptide 1- and 2-mediated uptake. J. Pharmacol. Exp. Ther. 299, 551–557.

Hagenbuch, N., Reichel, C., Stieger, B., Cattori, V., Fattinger, K.E., Landmann, L., Meier, P.J., Kullak-Ublick, G.A., 2001. Effect of phenobarbital on the expression of bile salt and organic anion transporters of rat liver. J. Hepatol. 34, 881–887.

Harrison, L.I., Gibaldi, M., 1976. Pharmacokinetics of digoxin in the rat. Drug Metab. Dispos. 4, 88–93.

Hassen, A.M., Lam, D., Chiba, M., Tan, E., Geng, W., Pang, K.S., 1996. Uptake of sulfate conjugates by isolated rat hepatocytes. Drug Metab. Dispos. 24, 792–798.

Hsiang, B., Zhu, Y., Wang, Z., Wu, Y., Sasseville, V., Yang, W.P., Kirchgessner, T.G., 1999. A novel human hepatic organic anion transporting polypeptide (OATP2). Identification of a liver-specific human organic anion transporting polypeptide and identification of rat and human hydroxymethylglutaryl-CoA reductase inhibitor transporters. J. Biol. Chem. 274, 37161–37168.

Keppler, D., Arias, I.M., 1997. Hepatic canalicular membrane. Introduction: transport across the hepatocyte canalicular membrane. FASEB J. 11, 15–18.

Kim, R.B., 2002. Transporters and xenobiotic disposition. Toxicology 182, 291–297.

Kopplow, K., Letschert, K., Konig, J., Walter, B., Keppler, D., 2005. Human hepatobiliary transport of organic anions analyzed by quadruple-transfected cells. Mol. Pharmacol. 68, 1031–1038.

Kwon, Y., Morris, M.E., 1997. Membrane transport in hepatic clearance of drugs. II. Zonal distribution patterns of concentration-dependent transport and elimination processes. Pharm. Res. 14, 780–785.

Lam, J.L., Benet, L.Z., 2004. Hepatic microsome studies are insufficient to characterize *in vivo* hepatic metabolic clearance and metabolic drug–drug interactions: studies of digoxin metabolism in primary rat hepatocytes versus microsomes. Drug Metab. Dispos. 32, 1311–1316.

Letschert, K., Komatsu, M., Hummel-Eisenbeiss, J., Keppler, D., 2005. Vectorial transport of the peptide CCK-8 by double-transfected MDCKII cells stably expressing the organic

anion transporter OATP1B3 (OATP8) and the export pump ABCC2. J. Pharmacol. Exp. Ther. 313, 549–556.
Lin, J.H., Wong, B.K., 2002. Complexities of glucuronidation affecting *in vitro in vivo* extrapolation. Curr. Drug Metab. 3, 623–646.
Liu, X., Chism, J.P., LeCluyse, E.L., Brouwer, K.R., Brouwer, K.L., 1999. Correlation of biliary excretion in sandwich-cultured rat hepatocytes and *in vivo* in rats. Drug Metab. Dispos. 27, 637–644.
Liu, L., Mak, E., Tirona, R.G., Tan, E., Novikoff, P.M., Wang, P., Wolkoff, A.W., Pang, K.S., 2005. Vascular binding, blood flow, transporter and enzyme interactions on the processing of digoxin in rat liver. J. Pharmacol. Exp. Ther. 315, 433–448.
Liu, L., Pang, K.S., 2005. The roles of transporters and enzymes in hepatic drug processing. Drug Metab. Dispos. 33, 1–9.
Maliepaard, M., Scheffer, G.L., Faneyte, I.F., van Gastelen, M.A., Pijnenborg, A.C., Schinkel, A.H., van De Vijver, M.J., Scheper, R.J., Schellens, J.H., 2001. Subcellular localization and distribution of the breast cancer resistance protein transporter in normal human tissues. Cancer Res. 61, 3458–3464.
Matsushima, S., Maeda, K., Kondo, C., Hirano, M., Sasaki, M., Suzuki, H., Sugiyama, Y., 2005. Identification of the hepatic efflux transporters of organic anions using double-transfected Madin-Darby canine kidney II cells expressing human organic anion-transporting polypeptide 1B1 (OATP1B1)/multidrug resistance-associated protein 2, OATP1B1/multidrug resistance 1, and OATP1B1/breast cancer resistance protein. J. Pharmacol. Exp. Ther. 314, 1059–1067.
Meier, P.J., 1996. Hepatocellular transport systems: from carrier identification in membrane vesicles to cloned proteins. J. Hepatol. 24 (Suppl. 1), 29–35.
Meier, P.J., Boyer, J.L., 1990. Preparation of basolateral (sinusoidal) and canalicular plasma membrane vesicles for the study of hepatic transport processes. Methods Enzymol. 192, 534–545.
Meier, P.J., Stieger, B., 2002. Bile salt transporters. Annu. Rev. Physiol. 64, 635–661.
Miller, R.E., Guengerich, F.P., 1983. Metabolism of trichloroethylene in isolated hepatocytes, microsomes, and reconstituted enzyme systems containing cytochrome P-450. Cancer Res. 43, 1145–1152.
Mistry, M., Houston, J.B., 1987. Glucuronidation *in vitro* and *in vivo*. Comparison of intestinal and hepatic conjugation of morphine, naloxone, and buprenorphine. Drug Metab. Dispos. 15, 710–717.
Mita, S., Suzuki, H., Akita, H., Stieger, B., Meier, P.J., Hofmann, A.F., Sugiyama, Y., 2005. Vectorial transport of bile salts across MDCK cells expressing both rat Na^+-taurocholate cotransporting polypeptide and rat bile salt export pump. Am. J. Physiol. Gastrointest. Liver Physiol. 288, G159–G167.
Mizuno, N., Niwa, T., Yotsumoto, Y., Sugiyama, Y., 2003. Impact of drug transporter studies on drug discovery and development. Pharmacol. Rev. 55, 425–461.
Möller, E., McIntosh, J.R., Van Slyke, D.D., 1929. Studies of urea excretion. J. Clin. Invest. 6, 427–465.
Noé, B., Hagenbuch, B., Stieger, B., Meier, P.J., 1997. Isolation of a multispecific organic anion and cardiac glycoside transporter from rat brain. Proc. Natl. Acad. Sci. U.S.A. 94, 10346–10350.
Obach, R.S., 1999. Prediction of human clearance of twenty-nine drugs from hepatic microsomal intrinsic clearance data: an examination of *in vitro* half-life approach and non-specific binding to microsomes. Drug Metab. Dispos. 27, 1350–1359.
Oinonen, T., Lindros, K.O., 1995. Hormonal regulation of the zonated expression of cytochrome P-450 3A in rat liver. Biochem. J. 309, 55–61.
Pang, K.S., 1995. Modeling of metabolite disposition. In: D'Argenio, D.Z. (Ed.), Advanced Methods of Pharmacokinetic and Pharmacodynamic System Analysis, vol. II. Plenum Press, New York, pp. 3–26.
Pang, K.S., Barker III, F., Cherry, W.F., Goresky, C.A., 1991. Esterases for enalapril hydrolysis are concentrated in the perihepatic venous region of the rat liver. J. Pharmacol. Exp. Ther. 257, 294–301.
Pang, K.S., Barker III, F., Simard, A., Schwab, A.J., Goresky, C.A., 1995. Sulfation of acetaminophen by the perfused rat liver: effect of red blood cell carriage. Hepatology 22, 267–282.
Pang, K.S., Chiba, M., 1994. Metabolism: scaling up from *in vitro* to organ and whole body. In: Welling, P.G., Balant, L.P. (Eds.), Handbook of Experimental Pharmacology. Springer-Verlag, Stuttgart, pp. 101–187.
Pang, K.S., Chung, A., Cui, Y., Keppler, D., 2002. Abolition of biliary excretion of enalapril and enalaprilat in EHBR perfused livers and enalapril is transported by OATP-2 and OATP-8, vol. 4, no. W4284. In: Proceedings of the AAPS Annual Meeting, November 12–14. AAPS. Pharm. Sci., Toronto.
Pang, K.S., Geng, W., Schwab, A.J., Goresky, C.A., 1998a. Probing the structure and function of the liver with the multiple indicator dilution technique. In: Bassingthwaigthe, J., Goresky, C.A., Lenihan, J.N. (Eds.), Whole Organ Approach to Cellular Metabolism: Capillary Permeation, Cellular Transport and Reaction Kinetics. Springer-Verlag, New York, pp. 325–368.
Pang, K.S., Lee, W.F., Cherry, W.F., Yuen, V., Accaputo, J., Fayz, S., Schwab, A.J., Goresky, C.A., 1988. Effects of perfusate flow rate on measured blood volume, disse space, intracellular water space, and drug extraction in the perfused rat liver preparation: characterization by the multiple indicator dilution technique. J. Pharmacokinet. Biopharm. 16, 595–632.
Pang, K.S., Rowland, M., 1977a. Hepatic clearance of drugs. I. Theoretical considerations of a "well-stirred" model and a "parallel tube" model. Influence of hepatic blood flow, plasma and blood cell binding, and the hepatocellular enzymatic activity on hepatic drug clearance. J. Pharmacokinet. Biopharm. 5, 625–653.
Pang, K.S., Rowland, M., 1977b. Hepatic clearance of drugs. II. Experimental evidence for acceptance of the "well-stirred" model over the "parallel tube" model using lidocaine in the perfused rat liver in situ preparation. J. Pharmacokinet. Biopharm. 5, 655–680.
Pang, K.S., Stillwell, R.N., 1983. An understanding of the role of enzyme localization of the liver on metabolite kinetics: a computer simulation. J. Pharmacokinet. Biopharm. 11, 451–468.
Pang, K.S., Terrell, J.A., Nelson, S.D., Feuer, K.F., Clements, M.J., Endrenyi, L., 1986. An enzyme-distributed system for lidocaine metabolism in the perfused rat liver preparation. J. Pharmacokinet. Biopharm. 14, 107–130.
Pang, K.S., Wang, P.J., Chung, A.Y., Wolkoff, A.W., 1998b. The modified dipeptide, enalapril, an angiotensin-converting enzyme inhibitor, is transported by the rat liver organic anion transport protein. Hepatology 28, 1341–1346.
Parkinson, A., 2001. Biotransformation of xenobiotics. In: Klaassen, C. (Ed.), Casarett and Doull's Toxicology. McGraw-Hill, Columbus, pp. 133–224.
Perl, W., Chinard, F.P., 1968. A convection-diffusion model of indicator transport through an organ. Circ. Res. 22, 273–298.
Roberts, M.S., Rowland, M., 1985. Hepatic elimination–dispersion model. J. Pharm. Sci. 74, 585–587.
Rowland, M., Benet, L.Z., Graham, G.G., 1973. Clearance concepts in pharmacokinetics. J. Pharmacokinet. Biopharm. 1, 123–136.
Salphati, L., Benet, L.Z., 1999. Metabolism of digoxin and digoxigenin digitoxosides in rat liver microsomes: involvement of cytochrome P4503A. Xenobiotica 29, 171–185.
Sasaki, M., Suzuki, H., Aoki, J., Ito, K., Meier, P.J., Sugiyama, Y., 2004. Prediction of *in vivo* biliary clearance from the *in vitro*

transcellular transport of organic anions across a double-transfected Madin-Darby canine kidney II monolayer expressing both rat organic anion transporting polypeptide 4 and multidrug resistance associated protein 2. Mol. Pharmacol. 66, 450–459.

Sasaki, M., Suzuki, H., Ito, K., Abe, T., Sugiyama, Y., 2002. Transcellular transport of organic anions across a double-transfected Madin-Darby canine kidney II cell monolayer expressing both human organic anion-transporting polypeptide (OATP2/SLC21A6) and multidrug resistance-associated protein 2 (MRP2/ABCC2). J. Biol. Chem. 277, 6497–6503.

Sato, H., Sugiyama, Y., Miyauchi, S., Sawada, Y., Iga, T., Hanano, M., 1986. A simulation study on the effect of a uniform diffusional barrier across hepatocytes on drug metabolism by evenly or unevenly distributed uni-enzyme in the liver. J. Pharm. Sci. 75, 3–8.

Schinkel, A.H., Wagenaar, E., van Deemter, L., Mol, C.A., Borst, P., 1995. Absence of mdr1a P-glycoprotein in mice affects tissue distribution and pharmacokinetics of dexamethasone, digoxin and cyclosporine A. J. Clin. Invest. 96, 1698–1705.

Sherman, I.A., Dlugosz, J.A., Barker, F., Sadeghi, F.M., Pang, K.S., 1996. Dynamics of arterial and portal venous flow interactions in perfused rat liver: an intravital microscopic study. Am. J. Physiol. 27, G201–G210.

Shitara, Y., Sugiyama, D., Kusuhara, H., Kato, Y., Abe, T., Meier, P.J., Itoh, T., Sugiyama, Y., 2002. Comparative inhibitory effects of different compounds on rat oatp1 (slc21a1)- and Oatp2 (Slc21a5)-mediated transport. Pharm. Res. 19, 147–153.

Sirianni, G.L., Pang, K.S., 1997. Organ clearance concepts: new perspectives on old principles. J. Pharmacokinet. Biopharm. 25, 449–470.

Soars, M.G., Burchell, B., Riley, R.J., 2002. *In vitro* analysis of human drug glucuronidation and prediction of *in vivo* metabolic clearance. J. Pharmacol. Exp. Ther. 301, 382–390.

Spears, K.J., Ross, J., Stenhouse, A., Ward, C.J., Goh, L.B., Wolf, C.R., Morgan, P., Ayrton, A., Friedberg, T.H., 2005. Directional trans-epithelial transport of organic anions in porcine LLC-PK1 cells that co-express human OATP1B1 (OATP-C) and MRP2. Biochem. Pharmacol. 69, 415–423.

Takasaki, S., Hano, H., 2001. Three-dimensional observations of the human hepatic artery (arterial system in the liver). J. Hepatol. 34, 455–466.

Tan, E., Pang, K.S., 2001. Sulfation is rate limiting in the futile cycling between estrone and estrone sulfate in enriched periportal and perivenous rat hepatocytes. Drug Metab. Dispos. 29, 335–346.

Thohan, S., Rosen, G.M., 2002. Liver slice technology as an *in vitro* model for metabolic and toxicity studies. Methods Mol. Biol. 196, 291–303.

Tirona, R.G., Kim, R.B., 2002. Pharmacogenomics of organic anion-transporting polypeptides (OATP). Adv. Drug Deliv. Rev. 54, 1343–1352.

Tirona, R.G., Pang, K.S., 1996. Sequestered endoplasmic reticulum space for sequential metabolism of salicylamide: coupling of hydroxylation and glucuronidation. Drug Metab. Dispos. 24, 821–833.

Tirona, R.G., Pang, K.S., 1999. Bimolecular glutathione conjugation of ethacrynic acid and efflux of the glutathione adduct by periportal and perivenous rat hepatocytes. J. Pharmacol. Exp. Ther. 290, 1230–1241.

Tirona, R.G., Tan, E., Meier, G., Pang, K.S., 1999. Uptake and glutathione conjugation kinetics of ethacrynic acid in rat liver: *in vitro* and perfusion studies. J. Pharmacol. Exp. Ther. 291, 1210–1219.

Trauner, M., Boyer, J.L., 2003. Bile salt transporters: molecular characterization, function, and regulation. Physiol. Rev. 83, 633–671.

Ullrich, D., Bock, K.W., 1984. Glucuronide formation of various drugs in liver microsomes and in isolated hepatocytes from phenobarbital- and 3-methylcholanthrene-treated rats. Biochem. Pharmacol. 33, 97–101.

Wilkinson, G.R., Shand, D.G., 1975. Commentary: a physiological approach to hepatic drug clearance. Clin. Pharmacol. Ther. 18, 377–390.

Winkler, K., Keiding, S., Tygstrup, N., 1973. Clearance as a quantitative measure of liver function. In: Paumgartner, P., Presig, R. (Eds.), The Liver: Quantitative Aspects of Structure and Functions. Karger, Basel, pp. 144–155.

Xu, X., Selick, P., Pang, K.S., 1993. Non-linear protein binding and enzyme heterogeneity: effects on hepatic drug removal. J. Pharmacokinet. Biopharm. 21, 43–74.

Zahlten, R.N., Stratman, F.W., 1974. The isolation of hormone sensitive rat hepatocytes by a modified enzymatic technique. Arch. Biochem. Biophys. 163, 606–608.